ISSN 0030-400X, Optics and Spectroscopy, 2019, Vol. 126, No. 5, pp. 574–579. © Pleiades Publishing, Ltd., 2019.
Russian Text © The Author(s), 2019, published in Optika i Spektroskopiya, 2019, Vol. 126, No. 5, pp. 656–662.

BIOPHOTONICS

Optical Properties of Human Eye Cataractous Lens in vitro in the Visible and Near-IR Ranges of the Spectrum[1]

A. V. Belikov[a], A. M. Zagorul'ko[b], S. N. Smirnov[a,*], A. N. Sergeev[a], A. A. Mikhailova[c], and A. A. Shimko[c]

[a] *St. Petersburg National Research University of Information Technologies, Mechanics and Optics (ITMO University), St. Petersburg, 197101 Russia*

[b] *Fedorov Eye Microsurgery Research and Technology Complex, St. Petersburg Branch, Ministry of Health of the Russian Federation, St. Petersburg, 192281 Russia*

[c] *Resource Center Optical and Laser Methods of Matter Research, St. Petersburg State University, St. Petersburg, 198504 Russia*

** e-mail: s.n.smirnov@inbox.ru*

Received January 8, 2019; revised January 24, 2019; accepted January 31, 2019

Abstract—The spectral dependences of the absorption coefficient, scattering coefficient, scattering anisotropy factor, and transport scattering coefficient for human eye lens in vitro at different stages of cataracts were studied. The spectra of the absorption coefficient and transport scattering coefficient were obtained for the spectral range 400–2300 nm, and the spectra of the scattering coefficient and the scattering anisotropy factor were obtained for the spectral range 400–1800 nm. The wavelength regions in which the spectra of the studied optical characteristics of human eye lens do not differ significantly and, conversely, differ significantly for the samples with different stages of cataract were identified.

DOI: 10.1134/S0030400X19050035

INTRODUCTION

Optimization of light exposure for the purposes of diagnosing, therapy, or surgery in ophthalmology is impossible without the full knowledge of the optical properties of the eye structures in health and disease. The development of modern methods of energy (including laser) cataract surgery requires a detailed study of the spectral dependences of the main optical characteristics of the lens of the human eye at different stages of cataract maturation, because they determine the adequacy of the choice of laser radiation parameters, which is the key factor that determines the success of laser cataract extraction.

The spectral properties of human and animal eye lenses in the normal state and their changes with aging have been well studied. The absorption spectrum of a normal monkey lens for the wavelength range from 300 nm to 5 μm is discussed in [1]. The optical properties of bovine and human eye lens were studied in [2] for wavelengths of 980, 1310, and 1530 nm. In [3], the optical coefficients of normal bovine eye tissues (including the lens) in the spectral range 750–1000 nm are reported. The spectral dependences of the scattering and absorption coefficients in normal bovine lens were obtained in [4] for three emission wavelengths of an Ar-laser (457.9, 488.0, and 514.5 nm). The collimated transmission spectra of the lens in the wavelength range 300–1100 nm, calculated for ordered and disordered scatterers, are presented in [5]. Experimental total transmission spectra of isolated aging and cataractous lens in the wavelength range 300–800 nm are discussed in [6]. In this case, the spectra are fairly similar, because it is difficult to detect the changes in the scattering properties of tissue by this measurement method, and the changes in the spectra can be attributed primarily to the changes in absorbance, which are more pronounced in the lens with black cataract [7]. The changes in the composition of scatterers and absorbers with age lead to significant differences in the scattering spectra of the lens [7]. The results of calculations for light backscattering and scattering at an angle of 90° in the wavelength range 300–1100 nm [8] qualitatively agree with the experimental data presented in [9].

The absorption spectra of the substances contained in the lens and the effect of changes in the concentration of these substances during the life on the absorption spectrum of the lens also discussed in the literature. The absorption spectra of an ageing lens protein,

[1] The 22nd Annual Conference Saratov Fall Meeting 2018 (SFM'18): VI International Symposium "Optics and Biophotonics" and XXII International School for Junior Scientists and Students on Optics, Laser Physics, and Biophotonics, September 24–29, 2018, Saratov, Russia.

as well as tryptophan and pigment 3-hydroxykynurenine-3-O-beta-glucoside (3-HKG), containing in the lens, are presented in [10]. It is shown, in particular, that the absorption bands of these substances are situated in the UV and visible regions of the spectrum. The absorption spectra of a normal monkey lens and an elderly human lens are discussed in [11]. The difference in the absorption spectra was found, which is explained by the change of the dominant chromophore of the lens substance with age: 3-HKG dominates in young lenses, whereas the senile (yellow) protein becomes the dominant chromophore with aging.

Despite the sufficiently large number of spectral studies, it should be noted that, unfortunately, the behavior of the main optical characteristics—the absorption coefficient (μ_a), the scattering coefficient (μ_s), the anisotropy factor (g), and the transport scattering coefficient (μ_s')—of human eye lens at different stages of cataract maturation in the infrared range is not fully understood. This particularly applies to the near-infrared range, which is of special interest because the radiation of lasers of this spectral range (Nd:YAG (λ = 1.44 μm) [12], Yb,Er:Glass (λ = 1.54 μm) [13], and femtosecond lasers with $\lambda \approx 1$ μm [14]) is widely used in the eye microsurgery and is very promising for laser cataract extraction.

This work is devoted to studying the behavior of the above-listed optical coefficients of human eye lenses at different stages of cataract maturity in the visible and near-infrared ranges of the spectrum.

MATERIALS AND METHODS

Human eye lenses for experimental studies were obtained during surgery on extracapsular cataract extraction. After removal from the eye cavity, the lenses were placed in a Viziton-PEG viscoelastic solution (OOO NEP MG, Russia) and stored for no more than 1 week in a refrigerator at approximately 4°C. Before the preparation of samples for spectrophotometric measurements, the lenses were carefully washed from the viscoelastic solution. The samples were thin sections 6.5 ± 0.3 mm in diameter, which were excised from the equatorial part of the lens with a Gillette Platinum Plus razor blade (Procter & Gamble, United States). The samples were divided into three groups depending on the stage (degree) of cataract maturation according to [15]: stage II (five samples), stage III–IV (eight samples), and stage V (five samples). The description of the lens samples prepared for spectroscopic studies is given in Table 1. The photographs of typical lens at the studied stages of cataract maturity are presented in Fig. 1.

Table 1. Description of the lens of the human eye in vitro samples for spectrophotometric studies

Sample no.	Section thickness, mm	Cataract maturity stage
1–5	1.55 ± 0.11	II
6–13	1.24 ± 0.08	III–IV
14–18	1.32 ± 0.13	V

Samples were fixed in a holder with minimal compression because it has a significant impact on the optical properties of the soft biological tissue studied [16]. The holder consisted of two slides (BK7), between which rubber gaskets (o-rings) were placed to support the sample and ensure its uniform clamping (Fig. 2). To prevent dehydration of the sample during measurements, the space between the rubber gasket and the sample was preliminarily filled with saline.

The total transmission and diffuse reflection coefficients of the samples were measured using a Lambda 1050 spectrophotometer (Perkin Elmer, Inc., United States) with an integrating sphere 150 mm in diameter. The spectral dependence of these coefficients was obtained in the wavelength range 400–2300 nm. The schemes of measurement of the total transmission and diffuse reflection are shown in Figs. 3a and 3b, respectively. The size of the incident light beam in these schemes was limited by diaphragm *2* and was 3.0 ± 0.1 mm.

The collimated transmission of the samples was also measured using a Lambda 1050 spectrophotometer (Perkin Elmer, Inc., United States) containing an aperture system in the measuring channel instead of the integrating sphere. The collimated transmission was measured in the range 400–1800 nm. The scheme of collimated transmission measurement is shown in

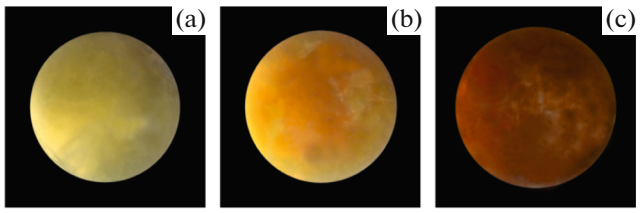

Fig. 1. Photographs of typical human eye lens in vitro: cataract stages (a) II, (b) III–IV, and (c) V. Frame size, 12 × 12 mm.

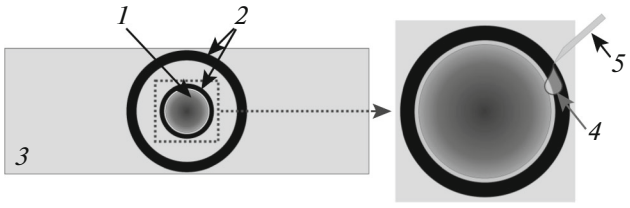

Fig. 2. Schematic representation of the sample holder. Designations: (*1*) sample (lens section), (*2*) rubber gaskets (o-rings), (*3*) slide, (*4*) saline, and (*5*) injection needle.

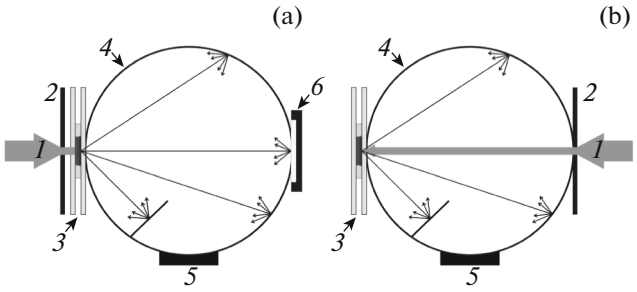

Fig. 3. Scheme of measuring of the total transmission (a) and diffuse reflection (b). Designations: (*1*) light beam, (*2*) circular aperture (diameter, 3 mm), (*3*) sample in the holder, (*4*) integrating sphere, (*5*) photodetector, and (*6*) reference scatterer.

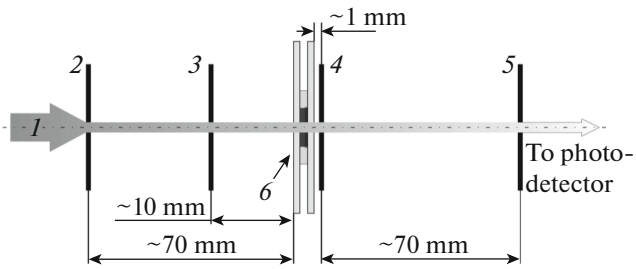

Fig. 4. Scheme of light beam orificing with change in collimated transmission. Designations: (*1*) light beam, (*2*, *3*, *4*, *5*) circular apertures (diameter, 2 mm), and (*6*) sample in the holder.

Fig. 4. The size of the incident light beam in this case was 2.0 ± 0.1 mm.

The selection of the wavelength range was determined by the high signal/noise ratio and as a result, the relatively small measurement error. Measurements in the range 400–850 nm were performed using a standard photomultiplier tube at a slit width of 2 nm. Measurements in the range 850–2300 nm were performed using a standard InGaAs detector in the Servo mode, which provided automatic selection of the slit width depending on the signal on the detector. Scanning was performed in increments of 2 nm.

All spectroscopic measurements were performed in the central region of the samples, and the beam offset from the center of the sample did not exceed 0.2 mm. For each sample, ten measurements were performed.

The diffuse reflection coefficients (R_d), the total transmission coefficient (T_t), and the collimated transmission coefficient (T_{cm}) of the samples formed the initial data set for further analysis. At the next stage, the data were processed using the IAD software (https://omlc.org/software/iad/), implementing the inverse adding–doubling (IAD) iterative method [17] for solving the inverse problem of radiative transfer. The IAD method is successfully used for processing the results of spectrophotometric measurements with the use of integrating spheres [18–20], and the calculation results in this approach do not depend on the ratio between the absorption and scattering coefficients of the sample [17]. Since the ratio of the absorption and scattering coefficients of cataractous lenses with different stages of cataracts in a wide range of wavelengths is unknown, the IAD method is the best to process the results.

As a result of processing, IAD software generates the spectral dependences of the absorption coefficient (μ_a) and the transport scattering coefficient (μ_s') of the samples. The transport scattering coefficient is determined by the following relation:

$$\mu_s' = \mu_s(1 - g), \quad (1)$$

where μ_s is the scattering coefficient and g is the scattering anisotropy factor.

When calculating μ_a and μ_s' values by the IAD method, the anisotropy scattering factor was taken to be $g = 0.8$, which is typical for the majority of biological tissues in the visible and near-infrared ranges of the spectrum [21]. Refractive index n of the lens was taken to be 1.4 [3, 4].

In the experiment, the diameter of the test sample was substantially greater than the size of the incident light beam on its surface. This made it possible to avoid errors in the determination of optical coefficients due to the scattered radiation loss through the sides of the sample [22].

The scattering anisotropy factor g was calculated on the basis of measured collimated transmission coefficient T_{cm}, and coefficients μ_a and μ_s', which were obtained in the previous step. According to the Bouguer–Lambert–Beer law, collimated transmission coefficient T_c is determined as follows:

$$T_c = \exp(-\mu_t l) = \exp(-(\mu_a + \mu_s)l), \quad (2)$$

where μ_t is the extinction coefficient, l is the thickness of the section (sample), μ_s is the scattering coefficient, and μ_a is the absorption coefficient.

To obtain collimated transmission coefficient T_c of the sample, it is necessary to correct measured collimated transmission coefficient T_{cm}, i.e., to take into account the losses associated with the reflection of light on the surfaces of slides between which the sample was fixed. The summary reflection coefficient for the air–glass–air system can be estimated as [23]

$$R = \frac{R_{ag} + R_{gs} - 2R_{ag}R_{gs}}{1 - R_{ag}R_{gs}}, \quad (3)$$

wherein R_{ag} is the Fresnel reflection coefficient at the air–glass interface and R_{gs} is the Fresnel reflection coefficient at the glass–sample interface.

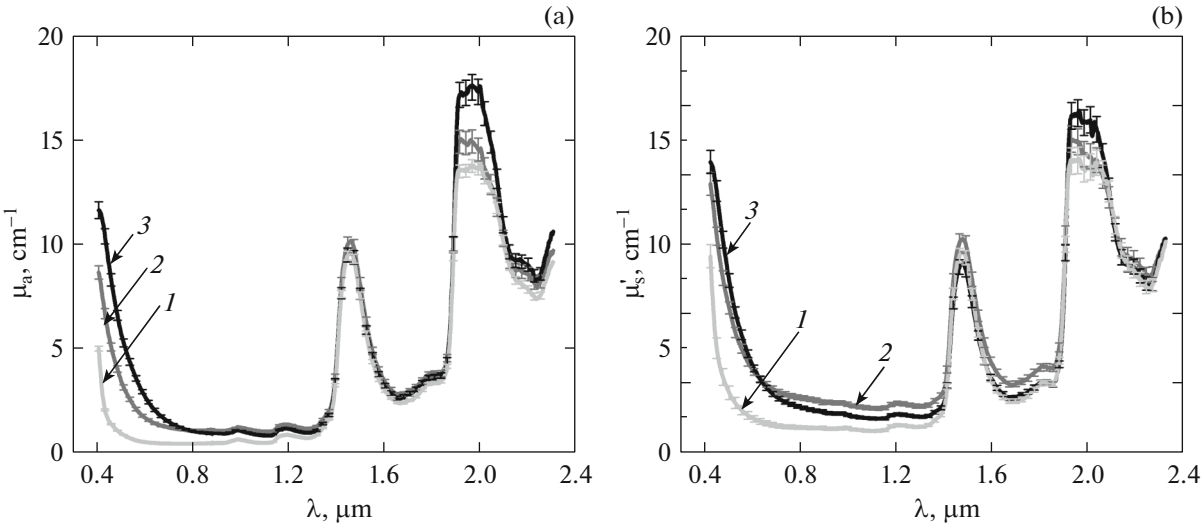

Fig. 5. Spectral dependences of (a) the absorption coefficient μ_a and (b) the transport scattering coefficient μ_s' of the samples of human eye lenses at different stages of a cataract in vitro. Designations: (*1*) stage II, (*2*) stage III–IV, and (*3*) stage V.

In this case, measured transmission coefficient T_{cm} is linked to collimated transmission coefficient T_c of the sample by the following expression [23]:

$$T_{cm} = \frac{(1-R)^2 T_c}{1 - R^2 T_c^2}. \quad (4)$$

Hence, the T_c coefficient can be expressed as

$$T_c = \frac{-(1-R)^2 - \sqrt{(1-R)^4 + 4R^2 T_{cm}^2}}{2T_{cm}R^2}. \quad (5)$$

Given (1) and (2), the following expression can be derived for the scattering anisotropy factor of the sample:

$$g = \frac{\mu_s'}{\frac{\ln(T_c)}{l} + \mu_a} + 1. \quad (6)$$

The results were statistically processed using the StatGraphics Plus software package (Statgraphics Technologies, Inc., United States). For the absorption coefficient (μ_a), the scattering coefficient (μ_s), the anisotropy factor (g), and the transport scattering coefficient (μ_s') of lenses, we calculated the mean value and the confidence interval for each spectral wavelength. The statistical significance of differences between the spectra of the above-listed optical coefficients obtained for the cataractous lenses with different stages of cataract was determined using the Kolmogorov–Smirnov test.

RESULTS AND DISCUSSION

The spectral dependences of the absorption coefficient (μ_a) and the transport scattering coefficient (μ_s') of human eye lens samples at different stages of cataract maturation, which were calculated using by the IAD method, are shown in Fig. 5.

The comparison of the spectral dependences of the absorption coefficient of the samples of cataractous lenses at stages II and III–IV using the Kolmogorov–Smirnov test showed that, in the entire spectral range studied, except λ = 2100–2125 nm, these spectra significantly differed from each other ($p < 0.05$). When the absorption spectra of the samples of cataractous lens at stages II and V were compared, statistically significant differences were also observed in the entire wavelength range studied, except the region λ = 1400–1500 nm; when samples at stages III–IV and V were compared, differences were significant over the entire wavelength range except λ = 760–785 nm and 1855–1890 nm.

The comparison of spectral dependences of the transport scattering coefficient of the samples of cataractous lenses at stages II and III–IV using the Kolmogorov–Smirnov test showed that, over the entire spectral range studied, except λ = 2100–2125 nm, these spectra significantly differed from each other ($p < 0.05$). When the spectra of the transport scattering coefficient of cataractous lens samples at stages II and V were compared, statistically significant differences were also observed in the entire wavelength range except λ = 1385–1395, 1530–1570, 1770–1850, and 2100–2300 nm; when samples at stages III–IV and V were compared, differences were significant over the entire wavelength range except λ = 590–620 and 2270–2300 nm.

The absorption spectrum of a cataractous lens in the visible region is determined primarily by the pigments that are derived from the amino acid tryptophan and accumulate with age and in cataract [24–26]. In

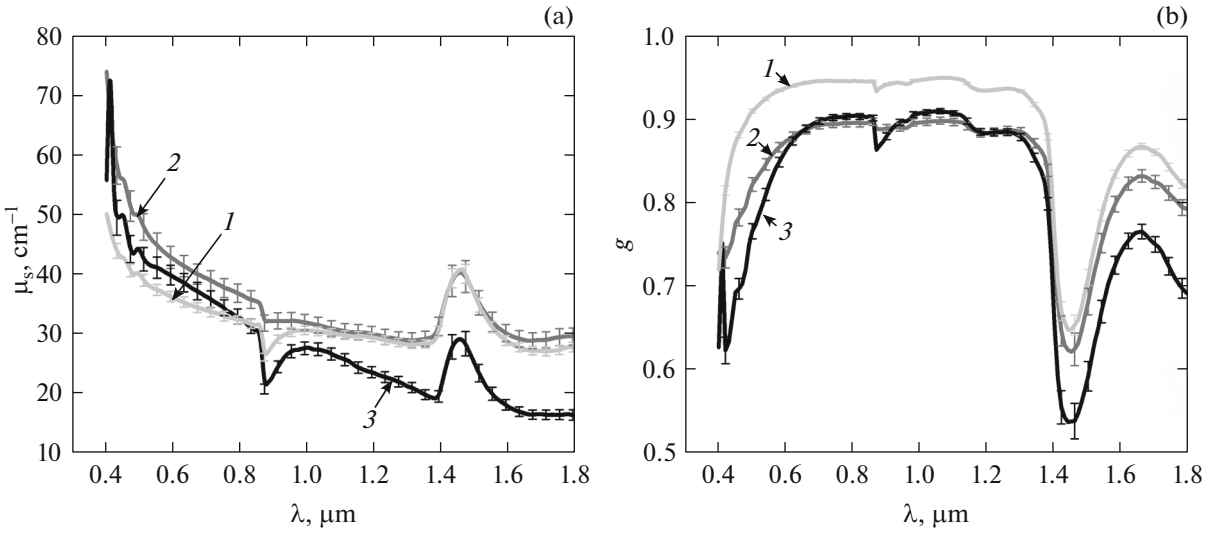

Fig. 6. Spectral dependences of (a) the scattering coefficient μ_s and (b) the scattering anisotropy factor g of the samples of human eye lens at different stages of a cataract in vitro. Designations: (*1*) stage II, (*2*) stage III–IV, and (*3*) stage V.

the near-infrared region, the absorption spectrum of the lens is determined by the free and bound water contained in it (the absorption peaks near 1450 and 1950 nm). The authors of [27] observed no significant changes in the water content in the human lens nucleus 13 to 82 years of age, may not be due to a cataract. In a cataract, the lens nucleus is compacted, and the content of bound water in it decreases [27, 28]. In the range 1900–2100 nm, spectra are distorted due to the nearly zero transmission of the samples, which results in a low signal/noise ratio. The high values of the transport scattering coefficient (μ_s') in both visible and near-infrared spectral regions are worth noting. The appearance of maxima in the μ_s' spectra in the near-infrared region, where intense water absorption bands are located, was also observed in [18]. According to the authors of [18], this effect may be associated with an increase in the imaginary part of the refractive index of the scatterers and the basic substance. This results in a significant decrease in the scattering anisotropy factor g, which, in particular, determines the transport scattering coefficient.

The spectral dependences of the scattering coefficient (μ_s) and the scattering anisotropy factor (g) of the samples of human eye lens with different stage of cataract, which were calculated using Eqs. (1) and (6), are shown in Fig. 6.

The distortion of the spectra in the region 850–980 nm may be associated with the use of different sensors at different wavelengths for recording the signal (a photomultiplier at $\lambda \le 850$ nm and an InGaAs photodetector at $\lambda > 850$ nm).

The comparison of the spectral dependences of the scattering coefficients of the cataractous lenses at stages II and III–IV using the Kolmogorov–Smirnov test showed that, over the entire spectral range except the region 1410–1520 nm, these spectra significantly differed from each other ($p < 0.05$). The spectral dependences of the scattering coefficient of the cataractous lenses at stages III–IV and V significantly differed from each other over the entire range ($p < 0.05$). When the absorption spectra of the cataractous lenses at stages II and V were compared, statistically significant differences were also observed in the entire wavelength range except $\lambda = 780$–830 nm.

The comparison of the spectral dependences of the anisotropy factor of the samples of cataractous lenses at stages II and III–IV and at stages II and V using the Kolmogorov–Smirnov test showed that these spectra significantly differed from each other over the entire range of the spectrum ($p < 0.05$). When comparing the absorption spectra of the anisotropy factor of the samples of cataractous lenses at stages III–IV and V, statistically significant differences were also observed in the entire wavelength range except $\lambda = 630$–680 and 1160–1280 nm.

The increase in the scattering coefficient of the cataractous lens upon the transition from stage II to V may be associated with the lens nucleus compaction. An increase in the lens nucleus rigidity with age was mentioned in [28, 29]. According to the authors of [30], the lens nucleus compaction may be due to the appearance of new fibers in the lens throughout life, as a result of which the old fibers are compressed at the center, as well as with an increase in the number of aggregated insoluble proteins. In the studied range (400–1800 nm), the dependence of the scattering coefficient on the wavelength did not decrease monotonically and had a maximum at the water absorption band with a center at approximately 1450 nm. A similar phenomenon was also noted by the authors of [31],

who explained it by the increase in the influence of the complex part of the refractive index of the scattering centers.

CONCLUSIONS

The optical properties of the human eye lens at different stages of cataract maturity were studied. The spectral dependences of the absorption coefficient (μ_a) and the transport scattering coefficient (μ_s') in the range 400–2300 nm, as well as the scattering anisotropy factor (g) and the scattering coefficient (μ_s) in the range 400–1800 nm, were obtained for the central part of the cataractous human eye lenses. It is found that, upon the transition of cataract from stage II to III–IV and then to V, the spectra of the above-listed optical coefficients of the lens significantly change, which should be taken into account when developing new methods for diagnosing, prevention, and treatment of cataracts.

ACKNOWLEDGMENTS

All measurements were performed at the Resource Center Optical and Laser Methods of Matter Research, St. Petersburg State University.

COMPLIANCE WITH ETHICAL STANDARDS

Conflict of interests. The authors declare that they have no conflict of interest.

Statement of compliance with standards of research involving human beings as subjects. All procedures performed in studies involving human participants were in accordance with the ethical standards of the institutional and/or national research committee and with the 1964 Helsinki Declaration and its later amendments or comparable ethical standards. Informed consent was obtained from all participants involved in the study.

REFERENCES

1. E. F. Maher, Report SAM-RT-78-32 (USAF School of Aerospace Medicine, 1978).
2. D. K. Sardar, R. M. Yow, G. -Y. Swanland, R. J. Thomas, and A. T. C. Tsin, Proc. SPIE **6138**, 613815 (2006).
3. B. G. Yust, L. C. Mimun, and D. K. Sardar, Lasers Med. Sci. **27**, 413 (2012).
4. D. K. Sardar, B. G. Yust, F. J. Barrera, L. C. Mimun, and A. T. C. Tsin, Lasers Med. Sci. **24**, 839 (2009).
5. V. V. Tuchin, I. L. Maksimova, V. I. Kochubey, T. N. Semenova, S. N. Tatarintsev, and N. L. Babkova, Proc. SPIE **2393**, 237 (1995).
6. V. V. Tuchin, I. L. Maksimova, A. N. Yaroslavskaya, T. N. Semenova, S. N. Tatarintsev, V. I. Kochubey, and V. F. Isotova, Proc. SPIE **2126**, 393 (1994).
7. V. V. Tuchin, *Lasers and Fiber Optics in Biomedical Research* (Fizmatlit, Moscow, 2010) [in Russian].
8. V. V. Tuchin and D. M. Zhestkov, Proc. SPIE **3053**, 123 (1997).
9. S. Zigman, G. Sutliff, and M. Rounds, Lens Eye Toxicity Res. **8**, 259 (1991).
10. J. Dillon, J. Photochem. Photobiol., B **10**, 23 (1991).
11. E. R. Gaillard, L. Zheng, J. C. Merriam, and J. Dillon, Invest. Ophthalmol. Visual Sci. **41**, 1454 (2000).
12. S. Yu. Kopaev, B. E. Malyugin, and V. G. Kopaeva, Oftal'mokhirurgiya, No. 4, 22 (2014).
13. A. V. Belikov, S. V. Gagarskii, A. B. Gubin, C. Ya. Vainer, A. N. Sergeev, and S. N. Smirnov, Nauch.-Tekh. Vestn. Inform. Tekhnol., Mekh. Opt. **15**, 1021 (2015).
14. K. E. Donaldson, R. Braga-Mele, F. Cabot, R. Davidson, D. K. Dhaliwal, R. Hamilton, M. Jackson, L. Patterson, K. Stonecipher, and S. H. Yoo, J. Cataract. Refract. Surg. **39**, 1753 (2013).
15. L. Buratto, *Phacoemulsification: Principles and Techniques* (SLACK Inc., Thorofare, NJ, 2003).
16. E. K. Chan, B. Sorg, D. Protsenko, M. O'Neil, M. Motamedi, and A. J. Welch, IEEE J. Sel. Top. Quant. Electron. **2**, 943 (1996).
17. S. A. Prahl, M. J. C. van Gemert, and A. J. Welch, Appl. Opt. **32**, 559 (1993).
18. A. N. Bashkatov, E. A. Genina, V. I. Kochubey, and V. V. Tuchin, J. Phys. D: Appl. Phys. **38**, 2543 (2005).
19. A. N. Bashkatov, E. A. Genina, V. I. Kochubey, and V. V. Tuchin, Opt. Spectrosc. **109**, 197 (2010).
20. A. N. Bashkatov, E. A. Genina, M. D. Kozintseva, V. I. Kochubei, S. Yu. Gorodkov, and V. V. Tuchin, Opt. Spectrosc. **120**, 1 (2016).
21. V. V. Tuchin, *Tissue Optics: Light Scattering Methods and Instruments for Medical Diagnosis* (SPIE Press, Bellingham, WA, 2007).
22. J. W. Pickering, S. A. Prahl, N. van Wieringen, J. F. Beek, H. J. C. M. Sterenborg, and M. J. C. van Gemert, Appl. Opt. **32**, 399 (1993).
23. V. I. Kochubei and A. N. Bashkatov, *Spectroscopy of Scattering Media* (Novyi Veter, Saratov, 2014) [in Russian].
24. M. P. Simunovic, Arch. Ophthalmol. **130**, 919 (2012).
25. S. Lerman, J. Gerontol. **38**, 293 (1983).
26. A. C. Sen, N. Ueno, and B. Chakrabarti, Photochem. Photobiol. **55**, 753 (1992).
27. N. Pescosolido, A. Barbato, R. Giannotti, C. Komaiha, and F. Lenarduzzi, Int. J. Ophthalmol. **9**, 1506 (2016).
28. K. R. Heys, PhD Thesis (Univ. Wollongong, 2010).
29. K. R. Heys, S. L. Cram, and R. J. Truscott, Mol. Vision **16**, 956 (2004).
30. H. Tabandeh, G. M. Thompson, and P. Heyworth, Eye **8**, 453 (1994).
31. A. N. Bashkatov, E. A. Genina, V. I. Kochubey, V. S. Rubtsov, E. A. Kolesnikova, and V. V. Tuchin, Quantum Electron. **44**, 779 (2014).

Translated by M. Batrukova